IEEE Access
Multidisciplinary | Rapid Review | Open Access Journal

Received 22 March 2023, accepted 7 April 2023, date of publication 12 April 2023, date of current version 17 April 2023.

Digital Object Identifier 10.1109/ACCESS.2023.3266722

RESEARCH ARTICLE

Mitigating Inaudible Ultrasound Attacks on Voice Assistants With Acoustic Metamaterials

JOSHUA S. LLOYD[1], COLE G. LUDWIKOWSKI[1], CYRUS MALIK[2], AND CHEN SHEN[1], (Member, IEEE)
[1]Department of Mechanical Engineering, Rowan University, Glassboro, NJ 08028, USA
[2]Department of Electrical and Computer Engineering, Rowan University, Glassboro, NJ 08028, USA

Corresponding author: Chen Shen (shenc@rowan.edu)

This work was supported by the National Science Foundation under Grant CMMI-2137749.

ABSTRACT Voice assistants play an important role in facilitating human–machine interactions and have been widely used in audio consumer electronic products. However, it has been shown that they are susceptible to inaudible attacks in which the malicious signals are in the ultrasound regime and cannot be heard by human ears. In this study, we show that a judiciously designed acoustic metamaterial filter can mitigate such attacks by modulating the received signals by the microphones. The metamaterial filter is composed of rigid plates with individual holes which exhibit local resonance phenomena that suppress incoming waves at specific frequencies. The effectiveness of the metamaterial filter is confirmed by experiments that show a combination of the holes can collectively distort the attack signals and protect the smart speakers. Moreover, normal audible signals are not affected by the proposed metamaterial, which adds to the flexibility of the device. The metamaterial filter has a small footprint and can be easily installed on various audio products. Our proposed strategy expands the capacity of acoustic metamaterials and improves the security of devices that use voice assistants.

INDEX TERMS Acoustic metamaterials, filters, ultrasound, voice assistants, wave propagation.

I. INTRODUCTION

Smart voice assistants have become a standard in most households in the last 5 years [1]. Devices such as computers, smartphones, and smart speakers all have voice assistants built-in to help complete tasks [2], [3]. Due to the great increase in their popularity, there also grows a concern for the exploitation of these devices [4], [5]. For example, voice assistants like Amazon Alexa have the ability to control locks on doors and garages, alarm systems, and other electronics in someone's home. In addition, these voice assistants can have access to one's personal information including address, contacts, and payment information. All these variables pose a potential threat if the voice assistant was ever exploited to give another person access to these features. It poses a danger to an individual's home security and cybersecurity.

One way of accomplishing the exploitation of voice assistants is by using ultrasonic commands [6], [7], [8]. These commands are outside of the audible range of humans; however, the microphones of these devices can still pick up the commands and execute them. This is because most microphones have an internal low-pass filter built into their hardware, with the cutoff usually being set at 20kHz to allow devices to operate in the audible frequency range. However, due to a "shadow" effect that occurs on the microphone diaphragm, inaudible frequencies are able to be processed as regular message signals, making any smart assistant vulnerable to inaudible attacks. While these ultrasonic attack signals can be defended against in a few ways, there does not exist a cost-effective solution that is efficient and robust in different conditions. For example, modifying the configuration of the hardware to include additional filters and circuits could potentially eliminate the shadow effect [9], [10]. This, however, requires additional components to the hardware and is complicated as the microphones are typically standardized. This drawback also applies to active noise control which allows selective filtering of ultrasonic frequencies but would be very costly and intrusive to realize [11], [12]. Modifying

The associate editor coordinating the review of this manuscript and approving it for publication was Ladislau Matekovits.

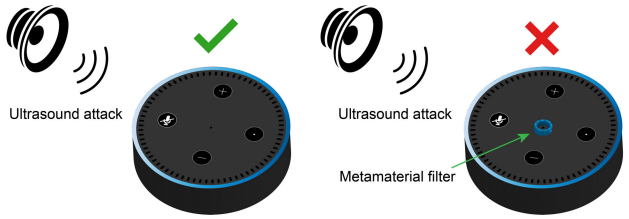

FIGURE 1. Conceptual illustration of ultrasound attacks on smart voice assistants. Malicious commands can be received and processed by voice assistants. When a metamaterial filter is installed, these inaudible signals are blocked and will not trigger the voice assistants.

the software, on the other hand, does not provide a permanent solution as the attack signals could also be modified to work through the new software defenses.

The advent of acoustic metamaterials opens the door for advanced manipulation of acoustic waves, which could address the aforementioned issues using physical structures. Acoustic metamaterials are artificially manufactured materials designed to control, direct, and manipulate sound waves [13], [14]. In particular, they have been developed to modulate acoustic waves within specific frequencies for various applications including noise control [15], [16], sensing [17], [18], [19], filtering [20], [21], energy harvesting [22], [23], and so on [24], [25], [26], [27], and [28]. While the realization of these unprecedented opportunities demonstrates a high degree-of-freedom offered by acoustic metamaterials, their usage in real devices and consumer products is less explored.

In this work, we develop a metamaterial-based approach to enhance the security of voice assistants. A composite acoustic metamaterial filter composed of rigid panels and individual resonators is designed that physically modifies ultrasonic attack signals so that they cannot trigger smart speakers. The proposed filters do not require any additional hardware to help prevent attack signals. They are small and can be conveniently installed on any smart speaker in order to operate. Measurements are performed on an Amazon Echo as an example to validate the proposed approach. When the metamaterial filters are installed, ultrasound attacks are effectively mitigated while normal audible signals can still be processed without any interruptions. Thanks to the relatively simple configuration, these filters can be reliably fabricated by additive manufacturing and can be produced with reduced cost for mass production. In comparison to other defense methods, the metamaterial filters provide a much simpler and more cost-efficient option. Our approach provides a versatile solution for sound filtering in audio devices and is expected to greatly reduce the risk of smart speakers being exploited by ultrasonic commands.

II. DESIGN AND SIMULATION

A. DESIGN OF THE ACOUSTIC METAMATERIAL FILTER

The concept of inaudible ultrasound attacks on voice assistants is illustrated in Fig. 1. Because of the "shadow" effect of the microphones, these voice assistants can pick up a specially modulated ultrasound signal containing information that can be further processed by them. This poses risks to the smart speaker as the ultrasound signals fall out of the audible spectrum and remain silent for humans, especially when malicious commands are employed. A carefully designed filter based on acoustic metamaterials can mitigate these attacks by filtering out the ultrasonic components while having minimum interruption to normal operations.

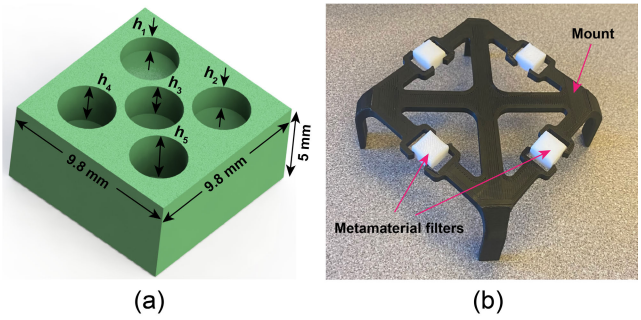

FIGURE 2. (a) Geometry of the proposed metamaterial filter. (b) A customized mount for the easy installation of the filters on smart speakers.

The schematic of the proposed acoustic metamaterial filters is shown in Fig. 2a. The metamaterial is composed of a rigid panel with dimensions 9.8 mm by 9.8 mm by 5.0 mm and several holes which act as Helmholtz-like resonators [29], [30]. The size of the panel is carefully chosen to fit over the casing of the smart speaker while being large enough to cover the microphone array in its entirety. The holes have a circular shape for the sake of simplicity and ease of fabrication. The radius of the holes is $r = 1.5$ mm and the depths h are h_1 through h_5. The resonance frequency of these resonators can be conveniently tuned by tailoring the depth of the holes. Meanwhile, the quality factor which determines the working bandwidth of the resonators depends on their radius. Because each resonator has a certain bandwidth and only reduces a particular frequency, multiple resonators were designed to form a composite filter to increase the effective frequency band within the ultrasound spectrum. Here, five individual holes with depths ranging from 1.0 mm to 3.0 mm are arranged on the square panel to collectively provide an acceptable filtering effect. As will be shown later, such a configuration can effectively filter out incoming acoustic waves within specific frequencies. A customized mount is further designed, as shown in Fig. 2b, so that the filters can be attached to it and installed on the smart speakers. It should be noted that a total number of four filters are attached. This is because the device we used (Amazon Echo Dot) has four microphones to locate the direction of the signals as well as to suppress background noise. Theoretically, the number of metamaterial filters should match the number of microphones used on a specific voice assistant to obtain the best performance.

B. NUMERICAL CHARACTERIZATION

To show the effectiveness of the metamaterial filter, numerical simulations based on finite element analysis using

COMSOL 5.6 are performed to evaluate its filtering performance. This is done by connecting the filters to a main waveguide and analyzing the corresponding transmission curves when the acoustic waves travel across the filter. In the simulations, the physical module of *Pressure Acoustics*, *Frequency Domain* is adopted. The simulations were run inside an air domain with perfectly matched layers placed at the end of the domain. The density and sound speed of air are set as 1.2 kg/m^3 and 343 m/s, respectively. Losses are considered in the simulations by using the built-in visco-thermal loss of the propagation medium. The filtering effect of a metamaterial filter containing single holes is first analyzed. Since the holes have a closed end at one side and are connected to the waveguide at the other side, the resonance frequency can be obtained by [31]:

$$f = \frac{c}{4(h + \Delta h)} \tag{1}$$

where $c = 343$ m/s is the sound speed in air and Δh is the end correction of the holes. The boundary condition is neither ideally flanged nor unflanged since the holes are connected to be confined space. Here, the end correction is estimated by numerical simulations [32] and is found to vary between $1.33r$ and $0.57r$ when the hole depth is changed from 0.5 mm to 4 mm. Fig. 3a depicts the resonance frequencies of the filters at different hole depths after obtaining the corresponding end corrections. Good agreement is found between the calculated and simulated values. The results provide a convenient means to determine the depths of the holes for the best filtering at desired center frequencies. On the other hand, the radii of the holes mainly affect the bandwidth of each individual resonator. For example, as illustrated in Fig. 3b, the relative filtering bandwidth is reduced by about 100% when the hole radius is varied from 2.1 mm to 0.9 mm with the hole depth being fixed to 2.0 mm. Changing the radius of the hole can also slightly shift the center frequency, which is mainly due to the variation of the end corrections. Together, the theoretical and numerical models serve as the basis for finding the best combination of geometric parameters of the metamaterial filter.

We then proceed to the composite metamaterial filters in which multiple holes are used to provide a strong filtering effect. Here the depths of the five holes are chosen to be 1.0 mm, 1.5 mm, 2.0 mm, 2.5 mm, and 3.0 mm, respectively, which prove to effectively filter out most of the ultrasonic frequencies in typical inaudible attacks, *e.g.*, within a frequency span between 20 kHz to 40 kHz as evidenced by Fig. 3a. The radius of the holes is set as 1.5 mm to provide sufficient filtering bandwidth while keeping the overall size of the holes compact to facilitate installation. As shown by Fig. 4a, each single resonator can only operate within a relatively small bandwidth. To enable the best filtering performance, a series of individual resonators are designed and arranged on the same panel. The collective resonance efficiently broadens the overall bandwidth of the metamaterial filter by introducing interactions among them [33], [34]. As a result, the

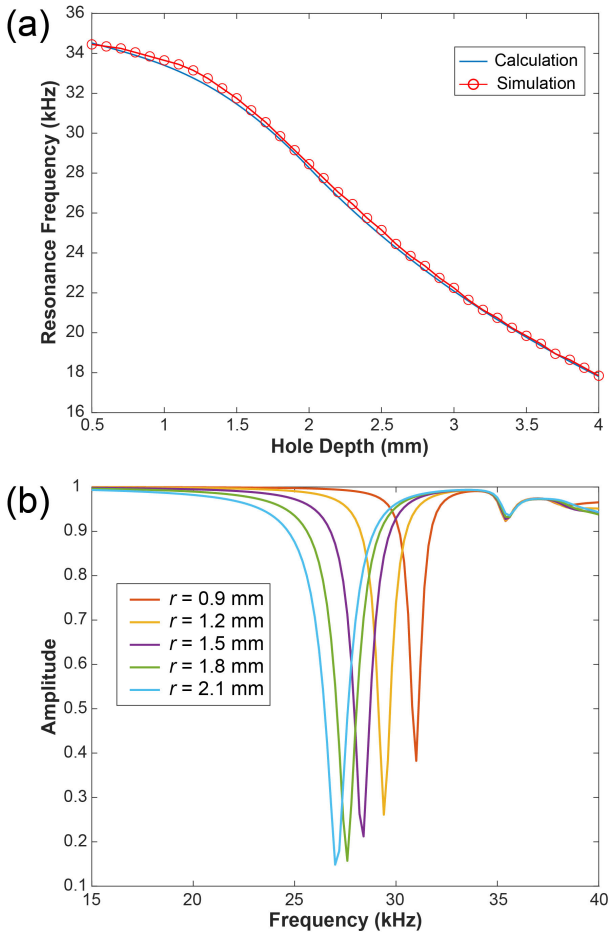

FIGURE 3. (a) Dependence of resonance frequency on the depth of the holes. (b) Dependence of filtering bandwidth on the radius of the holes.

transmission curve of the composite metamaterial exhibits a broadband filtering effect with well-defined troughs dictated by the individual resonators. It should be noted that some slight resonance frequency shift is observed for the metamaterial filter as compared to single resonators, which is likely to be caused by the mutual impedance among the holes as they are placed adjacent to each other [35]. In the meantime, the specific location of each hole is not expected to impact the overall filtering effect as long as they are compactly arranged. Figs. 4b-d depict the overall sound field distribution at three representative frequencies with an incident pressure amplitude of 1 Pa. The acoustic pressure field exhibits a low amplitude region near 30 kHz when the metamaterial filter is applied. On the other hand, waves below or near 20 kHz, which fall within the audible bands, are not much impacted by the metamaterial. The results demonstrate how the metamaterial filter can interact with the acoustic waves to greatly reduce the ultrasonic sound pressure near the microphone.

III. EXPERIMENT AND DISCUSSION

A. FABRICATION AND EXPERIMENTAL SETUP

After the structure of the metamaterial filters is designed, stereolithography (SLA) 3D printing was chosen as the best

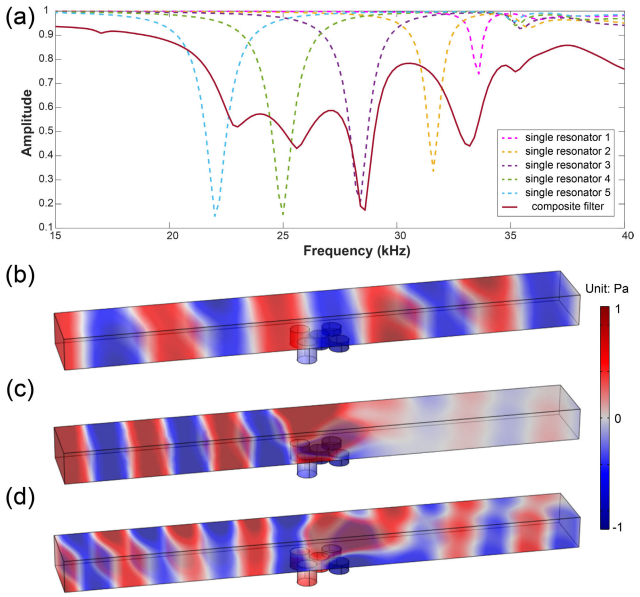

FIGURE 4. (a) Acoustic pressure received by the microphone when the metamaterial filter is absent. (b-d) Acoustic pressure distribution when the incident waves travel across the composite metamaterial filter at 20 kHz, 28.4 kHz, and 34 kHz.

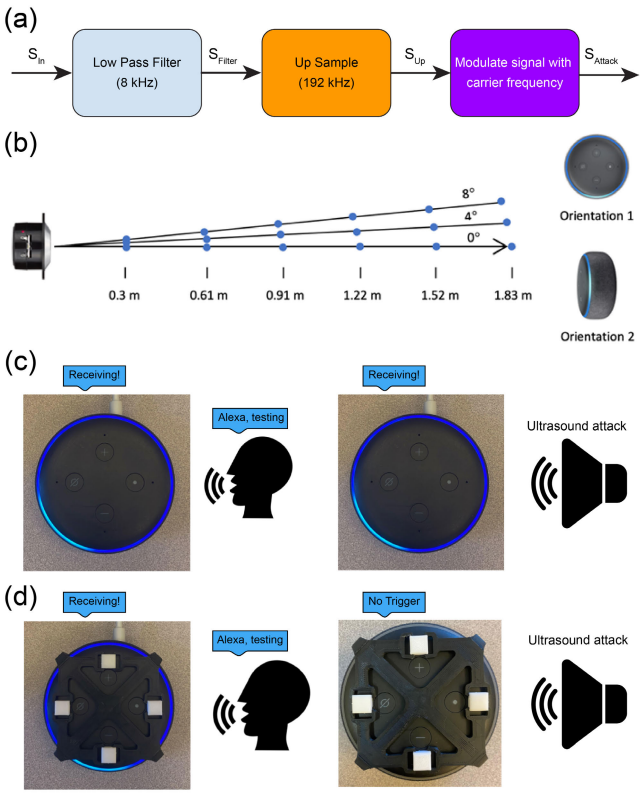

FIGURE 5. (a) Block diagram of inaudible ultrasound attack implementation. (b) Testing process diagram showing different configurations of the measurement setup. (c) Reactions from the smart speaker when the metamaterial filter is not installed. Both normal voice commands and ultrasonic signals are picked up by the speaker. (d) After the metamaterial filter is installed, only normal audible signals are processed while the ultrasound attacks are blocked.

method for prototype fabrication. A Formlabs Form 2 SLA 3D printer was used. The layer resolution is 100 microns and is much smaller than the smallest wavelength in this study. This produced accurate models without any noticeable surface roughness on the resonator walls, which ensures the performance of the filters.

To experimentally validate the proposed approach, measurements are first conducted to demonstrate attacks on voice assistants based on the shadow effect. This shadow effect concept is most easily understood by using two single tones. These two tones will generate frequencies that are equal to the sum and difference of the two tones when they vibrate the microphone [6]. For example, if two sine waves at 40 kHz and 50 kHz are played, they will yield frequencies at 10 kHz and 90 kHz at the microphone. The 90 kHz signal is still outside of the microphone's audible range, however, the 10 kHz is right in the middle of it, so the microphone will pick up the 10 kHz frequency. If amplitude modulation is further utilized with a message signal of 8 kHz and lower, a signal with a bandwidth of 16 kHz can be created. This yields frequencies in the audible range of 20 Hz to 16 kHz, which completely falls into the operating band of the microphone. Therefore, by utilizing amplitude modulation, a message signal which acts as the original command can be shifted into the ultrasonic range and can then be demodulated and interpreted by the microphone.

In order to test the effectiveness of the filters, an ultrasonic attack signal first needed to successfully be created and used on a smart speaker. The smart speaker chosen to test the attack signal was a third-generation Amazon Echo Dot. The ultrasound signals were obtained by modulating the regular voice commands and shifting them into the inaudible range to exploit the shadow effect [7]. Namely, we first applied a high-pass filter to the original audible audio file to eliminate unnecessary high-frequency components and then up-sample the file to 192kHz. Next, the audio is modulated into the ultrasonic frequency range and manipulated to take advantage of the aforementioned shadow effect. Due to the need for a very high sample rate, a Focusrite Scarlett Solo audio interface was used as the digital-to-analog converter (DAC). A dedicated high-resolution DAC, separate from the host computer, proved to be a key component in successfully sending an attack signal. This signal was sent to a Yamaha R-S202 for amplification, and then to a Fostex FT17H ultrasonic speaker. The use of the amplifier was important as it greatly increased the effective range of the attack signal. Finally, the attack signal was played from the ultrasonic speaker and received by the Echo Dot for various testing. Fig. 5a displays a block diagram of the steps taken in the code.

B. EXPERIMENTAL RESULTS

The main goal of our testing process was to use ultrasonic frequencies to activate an Amazon Echo Dot and determine the effectiveness of our defense method. First, our testing

criteria were expanded to include multiple smart speaker orientations, angles, and distances from the ultrasonic speaker. The Echo was tested both vertically (facing the ultrasonic speaker) and horizontally (lying flat on the table). Each of these orientations was also tested at an angle of 4 degrees and 8 degrees offset from the direct center of the ultrasonic speaker's throw. The distance between the smart speaker and ultrasonic speaker ranged from 0.3 m to 1.83 m, with each test increasing the distance by 0.31 m. Three trials were run at each distance, angle, and orientation, both with and without the filters placed on the Echo. Fig. 5b shows a visualization of the testing process.

When the Echo was in the vertical orientation, without filtering, it was triggered 100% of the time. At each distance, angle, and orientation the Echo was successfully triggered by the ultrasonic attack signal. When the filters were added, the Echo was never triggered by the attack signal, which results in a 100% success rate. For the horizontal orientation, without the filtering, it was able to be triggered 0.3 m away between zero and four degrees, and at 0.61 m between zero and four degrees. At these locations, the Echo was triggered 100% of the time by the attack signal. The triggering rate drops at larger angles and longer distances, which is caused by the high directivity of ultrasonic signals and the quick attenuation of acoustic energy at higher frequencies. When the filters were applied, the Echo was not activated during any test in the horizontal orientation. On the other hand, normal voice commands are not affected as the metamaterial filters operate mainly in the ultrasound regime, and the Echo responded in all of the configurations. Figs. 5c-d illustrate how the Amazon Echo interacted with the signals with and without the filters and show the different reactions with normal voice commands and ultrasonic signals. A video representation of the experiments can be found in the supplemental material.

To further characterize the filtering performance of the metamaterial, the received signal from the microphone was recorded to obtain its frequency spectrum. Pink noise was played 30 cm away from the microphone to include both audible and ultrasonic frequencies. This pink noise was then recorded both with and without a filter present. The results are summarized in Fig. 6. Fig. 6a shows the frequency response of the microphone without and with a filter. Fig. 6b plots the difference between each frequency response, indicated by the yellow overlay. It can be clearly seen that the filtering effect takes place mostly within the ultrasonic frequencies and does not much affect the audible components. Thanks to this selective filtering effect, the metamaterial filters effectively mitigate ultrasound attacks and present negligible impact on regular voice commands. It should be noted that, while all the measurements are done based on an Amazon Echo Dot as an example, the concept can be extended to accommodate other voice assistants and applications. For example, the size of the resonators can be conveniently adjusted to provide filtering at other specific frequency ranges. The solid panel and the mount can also be customized so that the filters can be installed on other products and devices. The number

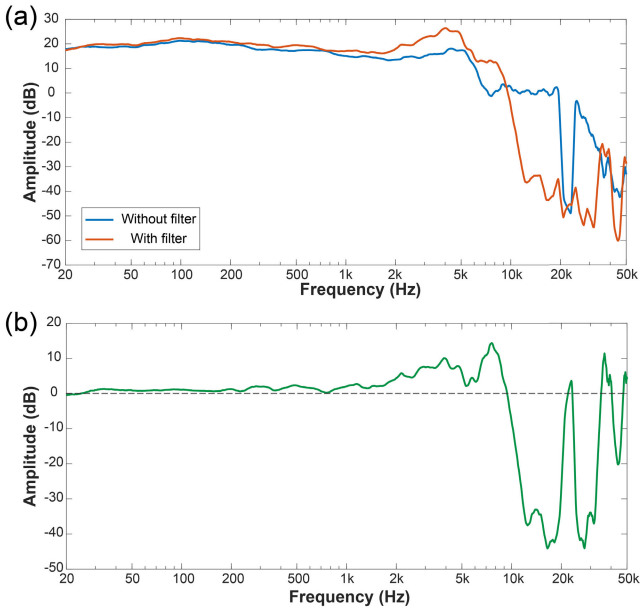

FIGURE 6. (a) Frequency spectrum of the received signals from the microphone without and with filters. (b) Net difference between the two cases. The reduction takes place mainly within the ultrasound frequencies.

of individual resonators depend on the specific application scenario and is chosen to be five to provide a relatively wide filtering bandwidth. This number may be reduced if a narrow frequency band needs to be filtered out. Overall, our proposed metamaterial filter exhibits great flexibility and customizability in protecting smart voice assistants.

IV. CONCLUSION

To conclude, we have successfully defended against an inaudible ultrasonic attack directed at manipulating smart speakers by utilizing a low-cost, composite metamaterial filter. The metamaterial filters act as small Helmholtz-like resonators designed to eliminate specific ultrasonic frequencies which could otherwise be used to silently attack a smart speaker. A straightforward design approach is presented by combining multiple resonators to broaden the bandwidth and achieve effective sound filtering. Measurements are performed to validate the proposed strategy. The results show that our metamaterials work as a functioning ultrasonic defense mechanism without noticeably affecting the audible frequency response when placed near a microphone. As a result, ultrasound attacks are effectively mitigated with the help of metamaterial filters. The metamaterials have a small size and can be conveniently installed on the exterior or the casing of the smart speakers, which adds great flexibility in terms of implementation. Although the smart speaker used extensively in our testing was an Amazon Echo Dot, this defense method could easily be applied to any smart speaker or voice assistant. Rather than modifying speaker hardware software, our filters provide a reliable, mechanical solution to an electrical problem. In principle, the operation bands of

the metamaterial can be tuned by modifying the dimensions and configuration of the resonators, which could further lead to selective filtering within desired frequency bands [36]. For example, one can tailor the center frequency and bandwidth of the filter by modifying the depth and radius of the corresponding holes. Moreover, the proposed structure can also be integrated with tunable components such as a screw-nut mechanism [37] or a fluid injection module [38] for reconfigurable filtering effects. Due to the simplicity of the design of our filters, it is envisioned that our proposed filters can be manufactured reliably in a low-cost manner to fit a large variety of applications.

ACKNOWLEDGMENT

The authors would like to thank Mark Butler, Evan Gould, Christopher Lentini, and Derek Phansalkar for their contributions during the early stage of this project. The authors Joshua S. Lloyd and Chen Shen are inventors on a pending U.S. provisional patent related to this work filed by Rowan University.

REFERENCES

[1] J. Humphry and C. Chesher, "Preparing for smart voice assistants: Cultural histories and media innovations," *New Media Soc.*, vol. 23, no. 7, pp. 1971–1988, Jul. 2021, doi: 10.1177/1461444820923679.

[2] F. Bentley, C. Luvogt, M. Silverman, R. Wirasinghe, B. White, and D. Lottridge, "Understanding the long-term use of smart speaker assistants," *Proc. ACM Interact., Mobile, Wearable Ubiquitous Technol.*, vol. 2, no. 3, pp. 1–24, Sep. 2018, doi: 10.1145/3264901.

[3] D. Pal, M. D. Babakerkhell, and X. Zhang, "Exploring the determinants of users' continuance usage intention of smart voice assistants," *IEEE Access*, vol. 9, pp. 162259–162275, 2021, doi: 10.1109/ACCESS.2021.3132399.

[4] J. S. Edu, J. M. Such, and G. Suarez-Tangil, "Smart home personal assistants: A security and privacy review," *ACM Comput. Surv.*, vol. 53, no. 6, p. 116, 2021, doi: 10.1145/3412383.

[5] C. Yan, X. Ji, K. Wang, Q. Jiang, Z. Jin, and W. Xu, "A survey on voice assistant security: Attacks and countermeasures," *ACM Comput. Surv.*, vol. 55, no. 4, p. 84, 2022, doi: 10.1145/3527153.

[6] N. Roy, H. Hassanieh, and R. Roy Choudhury, "BackDoor: Making microphones hear inaudible sounds," in *Proc. 15th Annu. Int. Conf. Mobile Syst., Appl., Services*, Jun. 2017, pp. 2–14, doi: 10.1145/3081333.3081366.

[7] G. Zhang, C. Yan, X. Ji, T. Zhang, T. Zhang, and W. Xu, "DolphinAttack: Inaudible voice commands," in *Proc. ACM SIGSAC Conf. Comput. Commun. Secur.*, Oct. 2017, pp. 103–117, doi: 10.1145/3133956.3134052.

[8] Q. Yan, K. Liu, Q. Zhou, H. Guo, and N. Zhang, "SurfingAttack: Interactive hidden attack on voice assistants using ultrasonic guided waves," in *Proc. Netw. Distrib. Syst. Secur. Symp.*, 2020, pp. 1–18, doi: 10.14722/ndss.2020.24068.

[9] V. Välimäki and J. D. Reiss, "All about audio equalization: Solutions and frontiers," *Appl. Sci.*, vol. 6, no. 5, p. 129, 2016.

[10] F. Wan, Z. Yuan, B. Ravelo, J. Ge, and W. Rahajandraibe, "Low-pass NGD voice signal sensoring with passive circuit," *IEEE Sensors J.*, vol. 20, no. 12, pp. 6762–6775, Jun. 2020, doi: 10.1109/JSEN.2020.2976531.

[11] S. M. Kuo and D. R. Morgan, "Active noise control: A tutorial review," *Proc. IEEE*, vol. 87, no. 6, pp. 943–973, Jun. 1999, doi: 10.1109/5.763310.

[12] L. Lu, K.-L. Yin, R. C. de Lamare, Z. Zheng, Y. Yu, X. Yang, and B. Chen, "A survey on active noise control in the past decade—Part I: Linear systems," *Signal Process.*, vol. 183, Jun. 2021, Art. no. 108039, doi: 10.1016/j.sigpro.2021.108039.

[13] S. A. Cummer, "Controlling sound with acoustic metamaterials," *Nature Rev. Mater.*, vol. 1, no. 3, 2016, Art. no. 16001, doi: 10.1038/natrevmats.2016.1.

[14] B. Assouar, B. Liang, Y. Wu, Y. Li, J.-C. Cheng, and Y. Jing, "Acoustic metasurfaces," *Nature Rev. Mater.*, vol. 3, no. 12, pp. 460–472, 2018, doi: 10.1038/s41578-018-0061-4.

[15] N. Gao, Z. Zhang, J. Deng, X. Guo, B. Cheng, and H. Hou, "Acoustic metamaterials for noise reduction: A review," *Adv. Mater. Technol.*, vol. 7, no. 6, Jun. 2022, Art. no. 2100698, doi: 10.1002/admt.202100698.

[16] S. Qu, N. Gao, A. Tinel, B. Morvan, V. Romero-García, J.-P. Groby, and P. Sheng, "Underwater metamaterial absorber with impedance-matched composite," *Sci. Adv.*, vol. 8, no. 20, May 2022, Art. no. eabm4206, doi: 10.1126/sciadv.abm4206.

[17] Z. Zhang, Y. Tian, Y. Wang, S. Gao, Y. Cheng, X. Liu, and J. Christensen, "Directional acoustic antennas based on valley-Hall topological insulators," *Adv. Mater.*, vol. 30, no. 36, Sep. 2018, Art. no. 1803229, doi: 10.1002/adma.201803229.

[18] T. Lee, T. Nomura, X. Su, and H. Iizuka, "Fano-like acoustic resonance for subwavelength directional sensing: 0–360 degree measurement," *Adv. Sci.*, vol. 7, no. 6, Mar. 2020, Art. no. 1903101, doi: 10.1002/advs.201903101.

[19] Y. Han, J. Chen, and Z. Fan, "Broadband characterization of near-field focusing with groove-structured lens," *IEEE Access*, vol. 9, pp. 46061–46067, 2021, doi: 10.1109/ACCESS.2021.3068319.

[20] H. Xinjing, Y. Yutian, M. Jinyu, L. Jian, and R. Xiaobo, "An acoustic metamaterial-based sensor capable of multiband filtering and amplification," *IEEE Sensors J.*, vol. 20, no. 8, pp. 4413–4419, Apr. 2020, doi: 10.1109/JSEN.2019.2962279.

[21] Y. Zhu, S.-W. Fan, L. Cao, K. Donda, and B. Assouar, "Acoustic meta-equalizer," *Phys. Rev. Appl.*, vol. 14, no. 1, Jul. 2020, Art. no. 014038, doi: 10.1103/PhysRevApplied.14.014038.

[22] S. Bansal, C. Choi, J. Hardwick, B. Bagchi, M. K. Tiwari, and S. Subramanian, "Transmissive labyrinthine acoustic metamaterial-based holography for extraordinary energy harvesting," *Adv. Eng. Mater.*, vol. 25, no. 4, Feb. 2023, Art. no. 2201117, doi: 10.1002/adem.202201117.

[23] X. Xu, Q. Wu, Y. Pang, Y. Cao, Y. Fang, G. Huang, and C. Cao, "Multifunctional metamaterials for energy harvesting and vibration control," *Adv. Funct. Mater.*, vol. 32, no. 7, Feb. 2022, Art. no. 2107896, doi: 10.1002/adfm.202107896.

[24] K. Yu, N. X. Fang, G. Huang, and Q. Wang, "Magnetoactive acoustic metamaterials," *Adv. Mater.*, vol. 30, no. 21, May 2018, Art. no. 1706348, doi: 10.1002/adma.201706348.

[25] L. Tong, Z. Xiong, Y. Shen, Y. Peng, X. Huang, L. Ye, M. Tang, F. Cai, H. Zheng, J. Xu, G. J. Cheng, and X. Zhu, "An acoustic meta-skin insulator," *Adv. Mater.*, vol. 32, no. 37, Sep. 2020, Art. no. 2002251, doi: 10.1002/adma.202002251.

[26] Z. Zhou, S. Huang, D. Li, J. Zhu, and Y. Li, "Broadband impedance modulation via non-local acoustic metamaterials," *Nat. Sci. Rev.*, vol. 9, no. 8, Sep. 2022, Art. no. nwab171, doi: 10.1093/nsr/nwab171.

[27] F. Mizukoshi and H. Takahashi, "A tunable open planar acoustic notch filter utilizing a pneumatically modulated Helmholtz resonator array," *IEEE Access*, vol. 10, pp. 118213–118221, 2022, doi: 10.1109/access.2022.3220366.

[28] G. Ji and J. Huber, "Recent progress in acoustic metamaterials and active piezoelectric acoustic metamaterials—A review," *Appl. Mater. Today*, vol. 26, Mar. 2022, Art. no. 101260, doi: 10.1016/j.apmt.2021.101260.

[29] Y. Xie, T.-H. Tsai, A. Konneker, B.-I. Popa, D. J. Brady, and S. A. Cummer, "Single-sensor multispeaker listening with acoustic metamaterials," *Proc. Nat. Acad. Sci. USA*, vol. 112, no. 34, pp. 10595–10598, Aug. 2015, doi: 10.1073/pnas.1502276112.

[30] Y. Zhu, X. Fan, B. Liang, J. Cheng, and Y. Jing, "Ultrathin acoustic metasurface-based schroeder diffuser," *Phys. Rev. X*, vol. 7, no. 2, Jun. 2017, Art. no. 021034, doi: 10.1103/PhysRevX.7.021034.

[31] L. E. Kinsler, A. U. Frey, A. B. Coppens, and J. V. Sanders, *Fundamentals of Acoustics*. New York, NY, USA: Wiley, 1982.

[32] C. Shen and Y. Jing, "Side branch-based acoustic metamaterials with a broad-band negative bulk modulus," *Appl. Phys. A, Solids Surf.*, vol. 117, no. 4, pp. 1885–1891, Dec. 2014, doi: 10.1007/s00339-014-8603-0.

[33] M. Yang, S. Chen, C. Fu, and P. Sheng, "Optimal sound-absorbing structures," *Mater. Horizons*, vol. 4, no. 4, pp. 673–680, 2017, doi: 10.1039/C7MH00129K.

[34] X. Peng, J. Ji, and Y. Jing, "Composite honeycomb metasurface panel for broadband sound absorption," *J. Acoust. Soc. Amer.*, vol. 144, no. 4, pp. EL255–EL261, Oct. 2018, doi: 10.1121/1.5055847.

[35] C. Shen, Y. Liu, and L. Huang, "On acoustic absorption mechanisms of multiple coupled quarter-wavelength resonators: Mutual impedance effects," *J. Sound Vibrat.*, vol. 508, Sep. 2021, Art. no. 116202, doi: 10.1016/j.jsv.2021.116202.

[36] C. Casarini, B. Tiller, C. Mineo, C. N. Macleod, J. F. C. Windmill, and J. C. Jackson, "Enhancing the sound absorption of small-scale 3-D printed acoustic metamaterials based on Helmholtz resonators," *IEEE Sensors J.*, vol. 18, no. 19, pp. 7949–7955, Oct. 2018, doi: 10.1109/JSEN.2018.2865129.
[37] S.-W. Fan, S.-D. Zhao, A.-L. Chen, Y.-F. Wang, B. Assouar, and Y.-S. Wang, "Tunable broadband reflective acoustic metasurface," *Phys. Rev. Appl.*, vol. 11, no. 4, Apr. 2019, Art. no. 044038, doi: 10.1103/PhysRevApplied.11.044038.
[38] Z. Tian, C. Shen, J. Li, E. Reit, Y. Gu, H. Fu, S. A. Cummer, and T. J. Huang, "Programmable acoustic metasurfaces," *Adv. Funct. Mater.*, vol. 29, no. 13, Mar. 2019, Art. no. 1808489, doi: 10.1002/adfm.201808489.

JOSHUA S. LLOYD is currently pursuing the degree in mechanical engineering with Rowan University.

He is interning with the Technical Training Development Department, Subaru of America. He is working on multiple engineering projects focused on improving class content for technicians. His research interests include acoustics, automotive engineering, and CAD modeling.

COLE G. LUDWIKOWSKI is currently pursuing the bachelor's degree in engineering with Rowan University. He was a Service Technician with Discount Pools and Supplies, Mount Holly, NJ, USA. His research interests include acoustics, CAD modeling, and autonomous systems.

CYRUS MALIK is currently pursuing the bachelor's degree in electrical and computer engineering with Rowan University. He was a full-time Intern with Power Systems Engineering Consulting Company, for two years. His research interests include power systems design, microprocessors, and acoustic filtering.

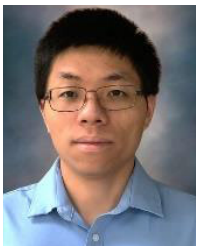

CHEN SHEN (Member, IEEE) received the B.S. degree from Nanjing University, in 2012, and the Ph.D. degree from North Carolina State University, in 2016. He is currently an Assistant Professor with the Department of Mechanical Engineering, Rowan University. His research interests include acoustic metamaterials, wave propagation, and acoustofluidics.